*Original Article*

JCBFM

Journal of Cerebral Blood Flow & Metabolism
2017, Vol. 37(5) 1670–1686

DOI: 10.1177/0271678X16657571
journals.sagepub.com/home/jcbfm
SAGE

# Altered hypermetabolic response to cortical spreading depolarizations after traumatic brain injury in rats

**Baptiste Balança[1,2], Anne Meiller[3], Laurent Bezin[1], Jens P. Dreier[4,5], Stéphane Marinesco[1,3,*] and Thomas Lieutaud[1,*]**

## Abstract

Spreading depolarizations are waves of near-complete breakdown of neuronal transmembrane ion gradients, free energy starving, and mass depolarization. Spreading depolarizations in electrically inactive tissue are associated with poor outcome in patients with traumatic brain injury. Here, we studied changes in regional cerebral blood flow and brain oxygen ($PbtO_2$), glucose ([Glc]b), and lactate ([Lac]b) concentrations in rats, using minimally invasive real-time sensors. Rats underwent either spreading depolarizations chemically triggered by KCl in naïve cortex in absence of traumatic brain injury or spontaneous spreading depolarizations in the traumatic penumbra after traumatic brain injury, or a cluster of spreading depolarizations triggered chemically by KCl in a remote window from which spreading depolarizations invaded penumbral tissue. Spreading depolarizations in noninjured cortex induced a hypermetabolic response characterized by a decline in [Glc]b and monophasic increases in regional cerebral blood flow, $PbtO_2$, and [Lac]b, indicating transient hyperglycolysis. Following traumatic brain injury, spontaneous spreading depolarizations occurred, causing further decline in [Glc]b and reducing the increase in regional cerebral blood flow and biphasic responses of $PbtO_2$ and [Lac]b, followed by prolonged decline. Recovery of $PbtO_2$ and [Lac]b was significantly delayed in traumatized animals. Prespreading depolarization [Glc]b levels determined the metabolic response to clusters. The results suggest a compromised hypermetabolic response to spreading depolarizations and slower return to physiological conditions following traumatic brain injury-induced spreading depolarizations.

## Keywords

Biosensors, brain trauma, brain metabolism, cerebral blood flow, energy metabolism, spreading depression, spreading depolarization

Received 5 February 2016; Revised 27 May 2016; Accepted 30 May 2016

## Introduction

Traumatic brain injury (TBI) induces widespread neuronal loss, with irreversible primary lesions directly induced by the trauma and secondary lesions that develop over time. It is assumed that the primary injury after TBI is surrounded by a hypoperfused zone with low concentrations of brain glucose ([Glc]b). In animal models of TBI, the majority of neurons in such zones die within a few days of the initial insult.[1–3] On computed tomography scans in patients, this area often shows hypodensity in acute and subacute stages and atrophy later on. On the basis of these observations, the concept of a pericontusional or traumatic "penumbra" was developed, by analogy with

[1]Inserm U1028, CNRS UMR 5292, Lyon Neuroscience Research Center, Team TIGER, Lyon, France
[2]Centre hospitalier universitaire de Lyon, France
[3]Université Claude Bernard Lyon I, Lyon Neuroscience Research Center, AniRA-Neurochem Technological platform, Lyon, France
[4]Center for Stroke Research Berlin, Charité University Medicine Berlin, Berlin, Germany
[5]Department of Neurology and Department of Experimental Neurology, Charité University Medicine Berlin, Berlin, Germany
*These authors contributed equally to this work.

**Corresponding author:**
Baptiste Balança, Lyon Neuroscience Research Center (CRNL), Team TIGER Universite Claude Bernard 8 Avenue, Rockefeller 69373, Lyon cedex 08, France.
Email: baptiste.balanca@gmail.com

the outer zone of focal cerebral ischemia.[4] In penumbral areas, onset of irreversible neuronal injury (''commitment point'') is reached later than in the inner zone, granting physicians more time to salvage.[5,6]

In addition to this state of hypoperfusion, another analogy between ischemic and traumatic penumbra is the occurrence of spreading depolarizations (SDs). SD is the generic term for waves of abrupt, sustained, near-complete breakdown of neuronal transmembrane ion gradients, free energy starving, and mass depolarization in the brain.[7–9] SDs can be recorded in about 56% of patients with severe TBI,[10,11] 60–70% of patients with intracerebral hemorrhage (ICH),[9] 70–80% of patients with poor-grade aneurysmal subarachnoid hemorrhage (aSAH),[12,13] and practically 100% of patients with malignant hemispheric stroke (MHS).[14,15] SDs result from acute increase in neuronal excitability and/or energy supply/demand mismatch.[16–20] They can trigger further neuronal injury through decreased perfusion (spreading ischemia)[11,21] and prolonged ionic imbalance.[6,7] In neurointensive care, clusters of SDs are increasingly considered as biomarkers that indicate disturbances in brain energy metabolism[12] and brain lesion development,[6] enabling prognostication and tailored therapy.[13,22]

However, a pathologically elevated oxygen extraction fraction (OEF), as defined in penumbral tissue in focal cerebral ischemia,[23,24] was not found within contusional or pericontusional tissue in patients with TBI.[25,26] The finding of hypoperfusion without concomitant increase in OEF in patients with TBI was similar to observations in patients with nontraumatic, supratentorial ICH.[27] The discrepancy between high OEF in oligemic tissue of the ischemic penumbra and low OEF in oligemic tissue of the traumatic penumbra suggests a difference in mechanism between these two types of penumbra.[26] Consequently, there is a need for better understanding of the biochemical processes that govern neuronal injury after TBI and of the mechanisms that differentiate traumatic from ischemic injury. Multimodal neuromonitoring, with cerebral microdialysis (cMD) catheters or sensors measuring partial pressure of brain tissue oxygen ($PbtO_2$) or regional cerebral blood flow (rCBF), is used for prognostication of outcome and therapeutic targeting in patients with TBI. These sensors are usually implanted in penumbral tissue.[28,29] In such studies, certain patterns of metabolic variables have been identified as potential biomarkers of long-term outcome. For example, increased lactate/glucose ratio (L/G) has been found in perilesional brain tissue and was associated with unfavorable outcome in patients with TBI.[30,31] In addition, ''metabolic crisis,'' defined by a high lactate/pyruvate ratio (L/P), was associated with poor prognosis.[32,33]

Metabolic crisis was further dichotomized based on brain lactate concentration ([Lac]b), rCBF, and $PbtO_2$: type 1 (ischemic) displays high [Lac]b whereas type 2 (nonischemic) displays normal to low [Lac]b.[32,33] By contrast, ''aerobic hyperglycolysis,'' defined as high [Lac]b and low L/P with rCBF and $PbtO_2$ within physiological ranges, was associated with good prognosis. These studies indicate that metabolic parameters such as brain glucose concentration ([Glc]b) or [Lac]b provide important information about the pathophysiological state of the underlying brain parenchyma.

The present study investigated the traumatic penumbra in rats, with a focus on the metabolic and vascular impact of SDs. For this purpose, we studied changes in cortical metabolism and brain supply of energy substrates during SDs in pericontusional temporal cortex after lateral fluid percussion injury (LFP injury) in an ipsilateral parietal cranial window. Specifically, we measured rCBF with laser-Doppler flowmetry (LDF), and $PbtO_2$, [Glc]b, and [Lac]b with minimally invasive real-time sensors under three conditions: rats underwent either SDs chemically triggered by KCl in naïve cortex in absence of TBI (control group), or developed spontaneous SDs in the traumatic penumbra after TBI (TBI-isolated group); in a third group, a cluster of SDs was triggered chemically after LFP injury using KCl in a remote window from which SDs invaded penumbral tissue (TBI-cluster group).

In naive brain, KCl-induced SDs were associated with a transient aerobic hyperglycolytic state. After TBI, the traumatic penumbra displayed a rapid decline in rCBF and [Glc]b. Spontaneous TBI-induced SDs in this area triggered metabolic and vascular responses indicating metabolic imbalance. This was even more pronounced during KCl-induced clusters of SDs.

## Methods

### Animals

Experiments were conducted in adult male Wistar rats of 250–400 g, supplied by Elevage Janvier (Le Genest Saint Isle, France). All experimental protocols were approved by the Claude Bernard Lyon-I University committee on animals in research (approval number: DR2014-31) and were performed in accordance with European directive 2010/63/EU, fulfilling the ARRIVE criteria. There was no significant difference in body weight between groups. Animals were housed in cages of four with a 12/12 h light–dark cycle and ad libitum food and water (AnimalerieRockfeller, Lyon France). Anesthesia started between 9 and 10 a.m. in all groups.

### Surgical preparation and TBI model

Nontraumatized animals (control group) remained in the stereotaxic frame, breathing spontaneously under light anesthesia (0.8–1.5% isoflurane in 30% oxygen with air). A 0.5 ml subcutaneous infiltration of 3 mg/ml ropivacaine (Naropeine; 7.5 mg/ml in saline) was performed prior to scalp incision. Circular craniotomy (5 mm diameter) centered 3.8 mm caudal to Bregma and 3.0 mm lateral to the midline was performed. Then, the dura was carefully removed, to avoid bleeding and enable probes to be inserted. The cranial window was rinsed with 0.9% saline at 2 ml/h.

Experimental animals were traumatized using a model of severe LFP injury.[2,3] Under isoflurane anesthesia, animals were intubated and artificially ventilated (Ispra MA1 55-7058, Harvard Apparatus$^{R}$, Edenbridge, UK; tidal volume = 6 ml/kg, breath rate = 60/min, positive end expiratory pressure = 5 cm $H_2O$). The same craniotomy procedure was performed as in control animals, and a hollow plastic cap was attached to the skull with cyanoacrylate and dental acrylic cement. A 1-mm-diameter stainless-steel screw inserted into the skull served as anchor. The animal was then removed from the stereotaxic frame and brought to the LFP-injury device (Custom Design and Fabrication, Virginia Commonwealth University, Richmond, VA). Rats received a single 20 ms fluid percussion pulse of 3.8 ATA under light anesthesia. This severe LFP injury produced a ~60% decrease in neuronal density in the temporal cortex lateral to the impact seven days after trauma (Figure 1(b)).[3] Without external intervention, this cortical area is therefore bound to degenerate and represents a traumatic penumbra. After LFP injury, animals were again placed in the stereotaxic frame under light anesthesia (0.8–1.5% isoflurane in 30% oxygen with air) for 5 h. Between 30 min and 1 h after LFP injury, arterial blood gas analysis was performed in nine animals under mechanical ventilation. The samples (200–400 µl) were analyzed with a GEM 300 device (Instrumentation Laboratory, Bedford, USA): pH = 7.35 [7.34;7.38], $PaO_2$ = 144 mmHg [136;149], $PaCO_2$ = 47 mmHg [44;51], $HCO_3^-$ = 25.5 mmol/l [24.7;26.8], Ht = 38% [34;41], and Hb = 11.8 g/dl [11.2;12.7]. Under these conditions, traumatized animals usually displayed isolated SDs and this group was therefore referred to as TBI isolated. A third group, in which a cluster of SDs was evoked by KCl apposition after TBI, was referred to as TBI cluster.

In all groups, animals' temperature was kept at 37°C with a homoeothermic blanket using a rectal temperature probe (Harvard Apparatus®, Edenbridge, UK). Oxygen saturation was monitored with a foot clip connected to a MouseOxPlus® system (Starr Life Sciences, Oakmont, PA), and arterial blood pressure via an arterial line equipped with a pressure sensor connected to a bioAmp amplifier (ADInstrument, Oxford, UK). At the end of the experiments, animals were euthanized with an intraperitoneal injection of sodium pentobarbital (150 mg/kg; Ceva, Libourne, France). In five LFP-injury animals, the brain tissue around the tip of a biosensor was electrocoagulated and the brain was then removed to confirm the cortical location of the biosensors.

### Probe placement

In the control group (naïve cortex), the LDF probe was placed on the exposed parietal cortex remote from larger vessels. A local field potential (LFP) electrode with either a $PbtO_2$ sensor or biosensors for [Glc]b and [Lac]b was inserted in deeper cortical layers between 500 and 1000 µm below the LDF probe.

In the TBI-isolated and TBI-cluster groups (severe TBI), the cranial bone overlying the temporal "traumatic penumbra" was thinned with a drill and the LDF probe was placed on the thinned bone under microscopic vision. Electrodes (i.e. LFP with either a $PbtO_2$ sensor or biosensors for [Glc]b and [Lac]b) were inserted through the cranial window made for the LFP injury, with a 25° angle so that the tips faced the LDF probe in deeper cortical layers similar to the control group.

*Experimental design.* We first assessed the general effect of LFP injury on rCBF, $PbtO_2$, [Glc]b, and [Lac]b, comparing changes from baseline in rCBF, $PbtO_2$, [Glc]b, and [Lac]b under two conditions: control group and TBI-isolated group. We then compared SDs evoked by KCl apposition in the control group to spontaneous SDs in the TBI-isolated group. In the control group, SDs were triggered at the recording site by a drop of KCl (1 mol/l) that was rapidly rinsed by a transient increase in the continuous saline flow (up to 5 ml/min for 1 min). Two SDs were triggered at least 30 min apart in each animal. In the TBI-isolated group, spontaneous SDs were recorded after severe LFP injury during the 30 min to 5 h posttrauma period (Figure 1(a)).

In the TBI-cluster group, we studied a KCl-induced cluster of recurrent SDs after LFP injury, by topical application of 1 mol/l KCl over the craniotomy. From this region, SDs invaded the temporal cortex (i.e. the traumatic penumbra) at a distance of 2 mm from the craniotomy site.

Twelve animals were included in each group (total = 36 animals): in six animals, rCBF and $PbtO_2$ were measured, and in the other six animals rCBF with [Glc]b and [Lac]b was measured using the respective biosensors. Thus, rCBF analysis was performed on

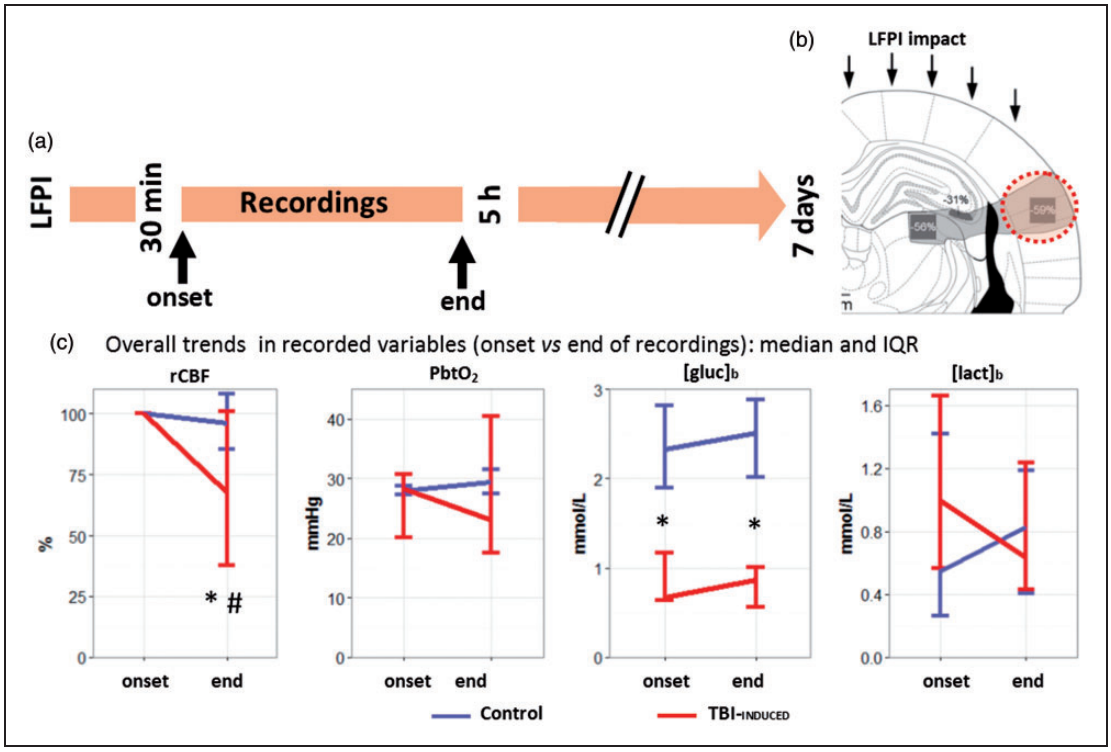


**Figure 1.** Trends of brain rCBF and metabolism during the recording period. (a) Experimental timeline after LFPI. Sensors were implanted in the temporal cortex, a brain area that undergoes a 60% decrease in neuronal density within the first seven days after LFPI (orange area in (b) adapted from Balança et al.[3] with permission). (c) Median and interquartile range (IQR) of regional cerebral blood flow (rCBF in %, n = 12 in both groups), brain tissue partial pressure of oxygen ($PbtO_2$ in mmHg, n = 6 in both groups), glucose and lactate extracellular brain concentrations ([Glc]b in mmol/l, n = 6 in both groups and [Lac]b in mmol/l, n = 6 in both groups), at the onset and the end of the recording period in control group (blue) and TBI-induced group (red). *$p \leq 0.05$, differences between groups, with a Wilcoxon rank sum test. #$p \leq 0.05$, difference between onset and end time point in the TBI-induced group, with a pairwise Wilcoxon rank sum test.

12 animals per group, and $PbtO_2$, cerebral metabolic rate of oxygen ($CMRO_2$), [Glc]b, and [Lac]b analyses were performed in six animals per group. Animals were included consecutively in the control, TBI-isolated, and TBI-cluster groups. Three more animals were included in the TBI-isolated group (total n = 15) but did not develop spontaneous SDs (20%). One animal developed a spontaneous cluster of recurrent SDs and was also included into the TBI-cluster group for [Glc]b and [Lac]b analysis.

*rCBF recording.* rCBF was recorded with a pencil LDF probe connected to a blood flowmeter (1 mm diameter tip, MNP100XP, ADInstrument, Oxford, UK). The probe was placed over the cortical surface, remote from larger vessels. rCBF was calculated as percentage change from baseline (=100%), measured during the first 5 min of each experiment. A zero level was established at the end of the experiments after euthanasia.

*SD detection.* LFP electrodes were made using Ag/AgCl wire inserted into a glass capillary with a pulled tip diameter of 3–5 µm (Harvard Apparatus, Edenbridge, UK), filled with a mix of 2 mol/l NaCl and 1 mol/l Na–citrate solution (1:1 ratio). A subcutaneous silver chloride reference was placed in the animal's neck. Signals were recorded by a near-DC octal bioAmp amplifier (ADInstrument, Oxford, UK) with built-in analog band-pass filter (0.02–100 Hz, sampling rate, 1 kHz). SDs were defined by the typical large slow change in potential, similar to clinical recordings using the same amplifier.[10] SDs were accompanied by spreading depression unless the spontaneous activity was already suppressed, as occurred in most experiments after TBI.

*$PbtO_2$ recording.* $PbtO_2$ recordings were made with an electrochemical (Clark-type) micro-sensor (10 µm tip; OX-10, Unisense, Aarhus, Denmark) connected to an amplifier with a constant potential of −800 mV. $PbtO_2$

electrodes were calibrated at 37°C before and after each experiment to convert the signal to mmHg.

### Biosensors for brain glucose and lactate recording

[Glc]b or [Lac]b concentrations were recorded using oxidase-based biosensors (tip: 100 µm in length and 40 µm in diameter; AniRA-Neurochem platform, Lyon, France). Briefly, biosensors were made using a Pt/Ir wire (Goodfellow, Huntington, UK) inserted into a pulled glass capillary (Harvard Apparatus, Edenbridge, UK). A poly-m-phenylenediamine (PPD) screening layer was deposited by electropolymerization and the enzyme layer was deposited by dipping the tip of the electrode into the enzyme solution: either glucose oxidase from *Aspergillus niger* (EC 1.4.3.11, Sigma-Aldrich, Saint Quentin Fallavier, France) or lactate oxidase from *Pediococcus* sp. (EC 1.13.12.4, Sigma-Aldrich, Saint Quentin Fallavier, France). Biosensors were covered with an additional polyurethane membrane to increase their dynamic range and to protect the enzyme layer from biofouling in the brain. Following this treatment, the dynamic range of Glc and Lac biosensors was 1.5 and 0.8 mM, respectively. Biosensors were connected to a VA-10 amplifier (NPI Electronics, Tamm, Germany) with a constant potential of +500 mV.[34] All sensors were tested in vitro before and after each in vivo experiment to ensure that sensitivity and specificity remained stable throughout the experiment. Only those sensitive enough (i.e. $\geq$50 pA/100 µM of glucose or lactate) with an effective PPD screening layer (i.e. <1.2 pA/20 µM response to serotonin) were used: roughly 90% of the microelectrodes.[34] Biosensors temperature and oxygen dependencies were studied in vitro and allowed us to correct the signal obtained in vivo to fit in vitro experimental conditions (i.e. 37 versus 25°C and 25–30 versus 159.6 mmHg). Therefore, brain concentrations were estimated using in vitro calibrations, taking account of the differences in temperature and oxygen concentrations measured with $PbtO_2$. The relationship between analyte concentration and oxidative current was modeled with a second-order polynomial function ($R^2 > 0.9$).

In 12 experiments (six controls and six LFP injury), the enzyme in the microelectrode biosensors was replaced by bovine serum albumin (BSA, Sigma-Aldrich, St Quentin Fallavier, France) to obtain control recordings of basal electrochemical (nonenzymatic) currents in the brain. These control biosensors, coated with albumin, recorded currents that were negligible compared to those with glucose or lactate oxidase. The small current changes detected on the BSA control electrodes were not taken into account for computing [Glc]b and [Lac]b.

A 16-bit PowerLab 16/35 was used as analog-to-digital converter. All signals were recorded and reviewed using LabChart 7 software (ADInstrument®, Oxford, UK). Biosensor, $PbtO_2$, and LDF signals were averaged each second.

### $CMRO_2$ calculation

$CMRO_2$ was computed off-line, second by second, from simultaneous $PbtO_2$ and LDF recordings, using the following formula, as in previous publications[35,36]

$$P_{bt}O_2 = P_{50} \cdot \sqrt[h]{\frac{2 \cdot Ca \cdot rCBF}{CMRO_2} - 1} - \frac{CMRO_2}{2 \cdot L}$$

Standard values of oxygen tension at hemoglobin half-saturation ($P_{50} = 34$ mmHg), and the Hill coefficient ($h = 2.7$) were used. The arterial content of oxygen, Ca, was 7.2 µmol/ml in our experiments. These values were combined with reported rCBF and $CMRO_2$ from the literature under isoflurane anesthesia (i.e. 135 ml/100 g/min and 357 µmol/100 g/min, respectively)[37] to calculate the corresponding effective diffusion coefficient of oxygen in brain tissue ($L = 510$ µmol/100 g/min/mmHg).

### Statistical analysis

Signal processing and statistical analysis were performed with R software (version 3.2.0, 2015-04-16, R Foundation for Statistical Computing, Vienna, Austria) using the additional libraries *signal*, *dplyr*, and *ggplot2*. Data are presented as median and interquartile range (IQR), and a p-value $\leq 0.05$ was considered significant. Since the LDF probe was placed with either $PbtO_2$ or biosensor probes, 12 animals in each group were included in the rCBF analyses whereas six in each group were included for $PbtO_2$, $CMRO_2$, [Glc]b, and [Lac]b analysis. To study the effect of LFP injury on isolated SDs, we compared control and TBI-isolated groups. rCBF, $PbtO_2$, $CMRO_2$, [Glc]b, and [Lac]b were analyzed in a time window from 10 min before to 20 min after each SD. The effect of TBI on these different parameters was analyzed by computing the area under the curve (AUC) during the 20 min following the start of the SD. Additionally, the time series were cut into 2 min epochs and compared on a repeated-measures ANOVA including both "time" and "group" as factors. Post hoc analysis on landmark values (e.g. min or max) and individual comparisons were made, by Wilcoxon rank sum test with Bonferroni correction, between groups. The effect of SD clusters after LFP injury was studied in the TBI-cluster group. rCBF,

$PbtO_2$, $CMRO_2$, [Glc]b, [Lac]b, and L/G values were analyzed with repeated-measures ANOVAs.

## Results

### Comparison between control and TBI-induced group

No significant difference was observed between the two groups regarding arterial blood glucose (7.3 mmol/l [6.4;9.3] versus 8.64 mmol/l [7.98;8.9], $p = 0.46$, $n = 6$ in both groups) or lactate (1.7 mmol/l [1.4;2.3] versus 1.7 mmol/l [1.68;1.99], $p = 0.96$, $n = 6$ in both groups). Systolic arterial pressure remained above 100 mmHg and arterial oxygen saturation ($SpO_2$) over 95% in both groups. There were no significant differences between baseline levels of $PbtO_2$, or [Lac]b, but [Glc]b was lower in the TBI isolated than the control group (0.67 mmol/l [0.63;1.17] versus 2.33 mmol/l [1.9;2.8], $n = 6$ in both groups, $p = 0.015$, Figure 1(c)). During the ~4.5 h recording period after LFP injury we were able to detect 2 [1.75;4] ($n = 12$: 6 with rCBF + $PbtO_2$ and 6 with rCBF + biosensors) spontaneous isolated SDs in 80% of the animals of the TBI-isolated group ($n = 12/15$). One spontaneous cluster was observed in one animal; isolated SDs also occurred in this animal and were included in the TBI-isolated group, while the cluster was included in the TBI-cluster group. In the TBI-isolated group, rCBF gradually declined during the experiment as a whole, reaching a level of 50.4% [28.1;86.5] ($n = 12$). By contrast, it remained stable in the control group ($n = 12$ in both groups, $p = 0.02$, Figure 1(c)). Unlike rCBF, $PbtO_2$, [Glc]b, and [Lac]b remained stable during the recording period (Figure 1(c)).

### Effect of isolated SDs in the control versus TBI-isolated group

Before each SD, rCBF (relative value compared to baseline) and [Glc]b (absolute value) were lower in the TBI-isolated group (68% [54.3;81.9] for LDF and 0.41 mmol/l [0.32;0.59] for [Glc]b) than in the control group (98.2% [92.39;118.4] for LDF, $p < 0.001$, $n = 12$, and 1.55 mmol/l [1.18;1.89], $p = 0.015$, $n = 6$, Figure 1). Pre-SD levels of $PbtO_2$ and [Lac]b did not differ between the two groups (Figures 1 and 2). The repeated-measures ANOVA performed on 2 min epochs of rCBF ($n = 12$ in both groups), $PbtO_2$ ($n = 6$), $CMRO_2$ ($n = 6$), [Glc]b ($n = 6$), and percentage [Lac]b variation ($n = 6$), indicated a significant interaction between the "*group*" and "*time*" factors (Figures 2 and 3).

Following SDs, rCBF displayed a transient increase in both groups (Figure 2) but the AUC was lower in the TBI-isolated group (61.2 s [34.6;88.7]) than in the control group (23.2 s [13.6;30.6]), $n = 12$, $p < 0.001$, Figure 2) indicating that the increase in rCBF was smaller after TBI.

In the control group, $PbtO_2$ transiently increased (+9 mmHg [5;11.7], AUC = 1304 mmHg s [806;2062], $p = 0.008$ versus zero, $n = 6$) at the same time as rCBF, whereas after LFP injury, SDs induced biphasic changes in $PbtO_2$ (Figure 2): the initial dip (−16.4 mmHg [−21.2;−12.3], $n = 6$) was not observed in control animals ($p = 0.001$, $n = 6$). However, this dip was followed by an increase in $PbtO_2$ that tended (non-significantly) to be higher than in the control group ($n = 6$, $p = 0.08$, Figure 2). The AUC was negative (−4998 mmHg s [−5432;−2692], $p = 0.006$ versus zero, $n = 6$) and significantly lower than in the control group ($p = 0.004$). $CMRO_2$ computed from rCBF and $PbtO_2$ transiently increased during SDs in both the control and the TBI-isolated group (Figure 2).

SDs induced a decrease in [Glc]b from 1.55 mmol/l [1.18;1.59] to 0.63 mmol/l [0.43;1.52] (i.e. −62.5% [−79.2;−51], $n = 6$) in the control group and from 0.41 mmol/l [0.32;0.59] to 0.2 mmol/l [0.167;0.242] (i.e. −67.2% [−80.7;−59.4], $n = 6$) in the TBI-isolated group (Figure 3). Since [Glc]b was always lower in the TBI-isolated group (Figure 3), the repeated-measures ANOVA performed on absolute values showed a significant "*group*" effect ($n = 6$ in both groups, $p = 0.002$, Figure 3). However, the relative change in [Glc]b evoked by SDs, expressed as percentage variation from the pre-SD [Glc]b level was non-significantly different between control and TBI animals (no "*group*" effect $n = 6$ in both groups, $p = 0.18$, Figure 3). The [Glc]b AUC were both different from zero ($n = 6$, $p < 0.05$ in both groups) but not different from one another. Thus, the relative pattern of [Glc]b changes was similar in control and TBI animals, but [Glc]b decreased to lower absolute values after TBI.

In the control group, [Lac]b showed a large increase, from 0.33 mmol/l [0.1;0.17] up to 2.25 mmol/l [0.55;5.91] (+168.7% [49.1;378.4], $n = 6$) whereas, in the TBI-isolated group, SDs induced a biphasic [Lac]b change. An initial dip (−70.4% [−87.4;−27.9], $n = 6$) was not observed in control animals ($p = 0.025$, $n = 6$) and was followed by a transient increase that was lower than in control animals (+19.2% [15.9;38.7], $n = 6$, $p = 0.04$, Figure 3). The [Lac]b AUC in the TBI group was significantly lower than zero (−192 mmol s [−460;−41], $n = 6$, $p = 0.03$), indicating a global decrease in [Lac]b. Moreover, the AUC in the TBI group was lower than in control animals (429 mmol s [19;1275], $n = 6$, $p = 0.015$). The heterogeneity in [Lac]b changes observed in the control group was likely responsible for the absence of a "*group*" effect ($n = 6$, $p = 0.13$, Figure 3). However, the ANOVA performed on 2 min epochs of the percentage variation from the

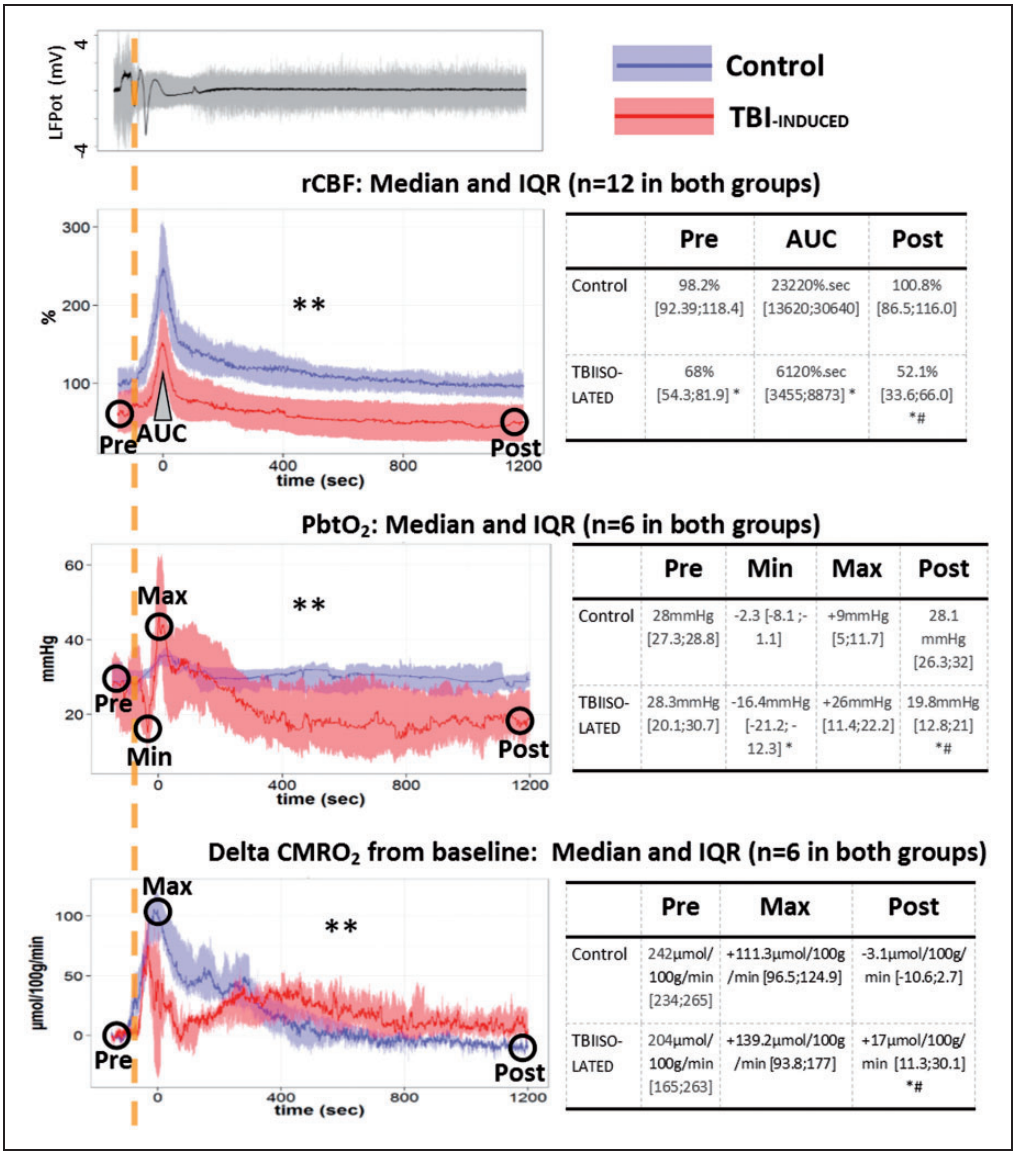


| | Pre | AUC | Post |
|---|---|---|---|
| Control | 98.2% [92.39;118.4] | 23220%.sec [13620;30640] | 100.8% [86.5;116.0] |
| TBIISO-LATED | 68% [54.3;81.9] * | 6120%.sec [3455;8873] * | 52.1% [33.6;66.0] *# |

| | Pre | Min | Max | Post |
|---|---|---|---|---|
| Control | 28mmHg [27.3;28.8] | -2.3 [-8.1 ;-1.1] | +9mmHg [5;11.7] | 28.1 mmHg [26.3;32] |
| TBIISO-LATED | 28.3mmHg [20.1;30.7] | -16.4mmHg [-21.2; -12.3] * | +26mmHg [11.4;22.2] | 19.8mmHg [12.8;21] *# |

| | Pre | Max | Post |
|---|---|---|---|
| Control | 242µmol/100g/min [234;265] | +111.3µmol/100g/min [96.5;124.9] | -3.1µmol/100g/min [-10.6;2.7] |
| TBIISO-LATED | 204µmol/100g/min [165;263] | +139.2µmol/100g/min [93.8;177] | +17µmol/100g/min [11.3;30.1] *# |

**Figure 2.** Changes of rCBF, $PbtO_2$, and $CMRO_2$ during the first 20 min following isolated SDs in normal and injured brain. An original local field potential (LFPot) recording of an SD example is given in the top left panel, showing a characteristic slow potential change in the near-DC electrocorticogram (black curve, bandpass: 0.02–0.5 Hz). SD typically induces spreading depression of spontaneous activity in electrically active tissue which is observed in the AC frequency range above 0.5 Hz (gray curve). The dashed orange vertical line marks the onset of SD. Changes of regional cerebral blood flow (rCBF in %, n = 12 in both groups), brain tissue partial pressure of oxygen ($PbtO_2$ in mmHg, n = 6 in both groups), and cerebral metabolic rate of oxygen ($CMRO_2$ in µmol/100 g/min, n = 6 in both group), are plotted over time on the left (median and IQR) in the control (blue) and TBI-induced (red) groups. SDs induced a transient increase in rCBF and $CMRO_2$ in both groups. $PbtO_2$ increased during SD in the control group whereas it showed a biphasic response with initial decline followed by increase in the TBI-induced group. Tables on the right provide the values before (**Pre**) and 20 min after (**Post**) SD, as well as the area under the curve (**AUC**) of the hyperemic rCBF response and minimum (**Min**) and maximum (**Max**) changes of $PbtO_2$ and $CMRO_2$. ** $p \leq 0.01$: interaction between "*time*" and "*group*" factors in a repeated measures ANOVA performed on 2 min epochs. * $p \leq 0.05$, differences between groups, with a Wilcoxon rank sum test. # $p \leq 0.05$, difference between pre- and posttime point, with a pairwise Wilcoxon rank sum test.

pre-SD [Lac]b level showed different temporal evolution in the two groups (significant interaction between "*group*" and "*time*," n = 6, p = 0.03, Figure 3).

Twenty minutes after SD, rCBF, $PbtO_2$, $CMRO_2$, [Glc]b, and [Lac]b had recovered to their pre-SD values in the control group (Figures 2 and 3). In the TBI-isolated group, rCBF, $PbtO_2$, and [Lac]b remained lower than their pre-SD levels at the end of the 20 min recording session. $CMRO_2$ remained at +17 µmol/100 g/min [11.3;30.1] above its pre-SD value

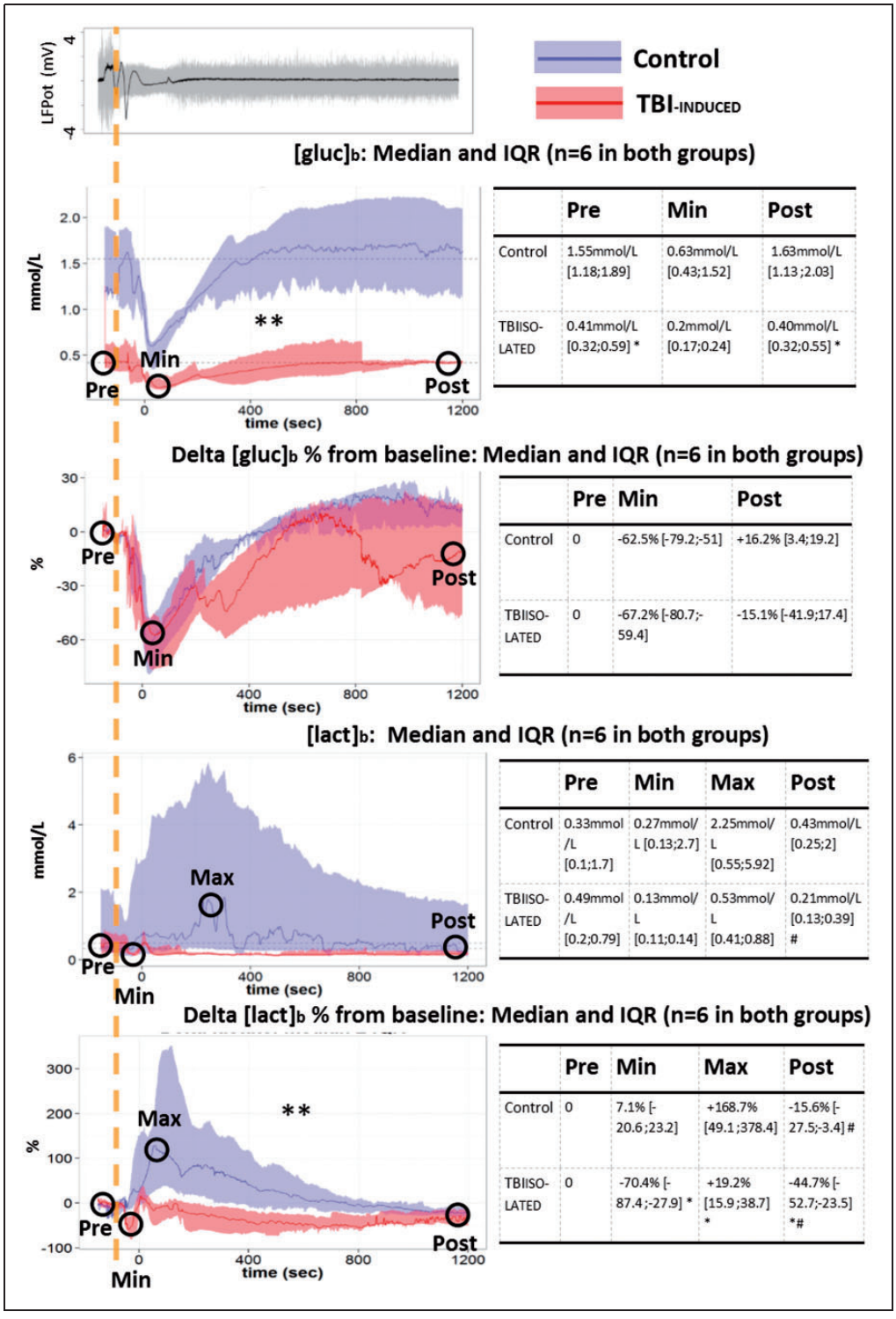


| | Pre | Min | Post |
|---|---|---|---|
| Control | 1.55mmol/L [1.18;1.89] | 0.63mmol/L [0.43;1.52] | 1.63mmol/L [1.13 ;2.03] |
| TBIISO-LATED | 0.41mmol/L [0.32;0.59] * | 0.2mmol/L [0.17;0.24] | 0.40mmol/L [0.32;0.55] * |

| | Pre | Min | Post |
|---|---|---|---|
| Control | 0 | -62.5% [-79.2;-51] | +16.2% [3.4;19.2] |
| TBIISO-LATED | 0 | -67.2% [-80.7;-59.4] | -15.1% [-41.9;17.4] |

| | Pre | Min | Max | Post |
|---|---|---|---|---|
| Control | 0.33mmol/L [0.1;1.7] | 0.27mmol/L [0.13;2.7] | 2.25mmol/L [0.55;5.92] | 0.43mmol/L [0.25;2] |
| TBIISO-LATED | 0.49mmol/L [0.2;0.79] | 0.13mmol/L [0.11;0.14] | 0.53mmol/L [0.41;0.88] | 0.21mmol/L [0.13;0.39] # |

| | Pre | Min | Max | Post |
|---|---|---|---|---|
| Control | 0 | 7.1% [-20.6;23.2] | +168.7% [49.1;378.4] | -15.6% [-27.5;-3.4] # |
| TBIISO-LATED | 0 | -70.4% [-87.4;-27.9] * | +19.2% [15.9;38.7] * | -44.7% [-52.7;-23.5] *# |

**Figure 3.** Changes of [Glc]b and [Lac]b during the first 20 min following isolated SDs in normal and injured brain. Top left panel shows SD and spreading depression similar to Figure 2 (gray curve). Absolute changes of extracellular brain glucose ([Glc]b in mmol/l, n = 6 in both groups) and lactate([Lac]b in mmol/l, n = 6 in both groups) and relative changes (% from pre-SD concentration) are plotted over time on the left. Tables on the right provide values before (**Pre**) and 20 min after SD (**Post**), as well as the minimum (**Min**) and maximum values (**Max**). Relative changes of [Glc]b were not different between the two groups in contrast to the absolute values whereas relative changes of [Lac]b were different between the two groups but not the absolute values. A biphasic [Lac]b response reminiscent of the $PbtO_2$ response in Figure 2 was observed only in the TBI-induced group. **$p \leq 0.01$: interaction between "*time*" and "*group*" factors with a repeated measures ANOVA performed on 2 min epochs. *$p \leq 0.05$, differences between groups, with a Wilcoxon rank sum test. #$p \leq 0.05$, difference between pre- and posttime point, with a pairwise Wilcoxon rank sum test.

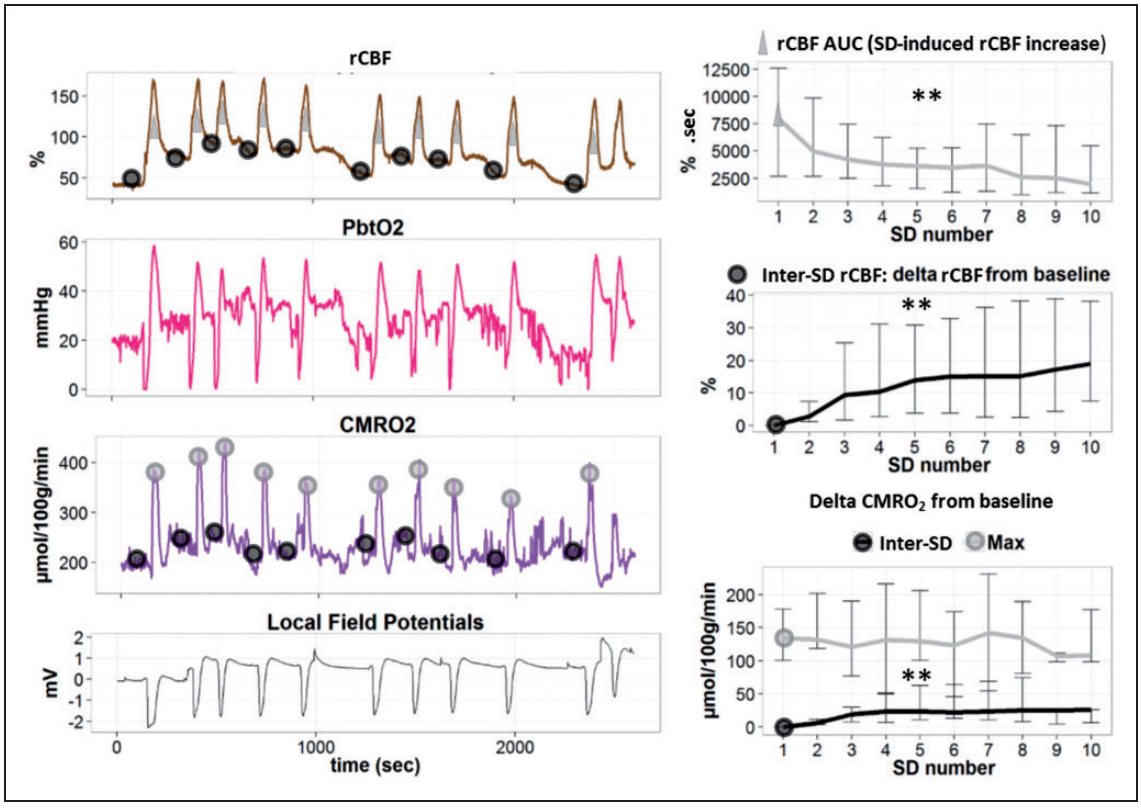


**Figure 4.** Changes of rCBF and metabolic variables during clusters of SDs in the injured brain. Left panel: regional cerebral blood flow (rCBF in %), brain tissue partial pressure of oxygen ($PbtO_2$ in mmHg), cerebral metabolic rate of oxygen ($CMRO_2$ in µmol/100 g/min), and local field potentials (LFPot in mV), during a cluster of SDs (original traces). Black circles describe the points for calculations of baseline and inter-SD values of rCBF and $CMRO_2$. Gray triangles and circles, respectively, describe the points for the calculations of the area under the curve (AUC) (rCBF increase) and the maximum (Max) of $CMRO_2$. Right panel: rCBF AUC and inter-SD rCBF (median and IQR, n = 12) are presented as percentage change from baseline (precluster). Note that rCBF AUC decreased while the inter-SD rCBF level increased during the cluster. In the right lower panel, maximum (Max) and inter-SD $CMRO_2$ (Median and IQR, n = 6) relative to baseline show a constant peak with a gradual increase of inter-SD $CMRO_2$ during the cluster. ** $p \leq 0.01$: effect of "*SD number*" factor in a repeated measures ANOVA.

(n = 6, p = 0.04). By contrast, [Glc]b returned to its pre-SD concentration within about 10 min, similarly to control animals (Figures 2 and 3). These data indicate a slower return to baseline metabolic values after TBI.

## *Effect of SD clusters after LFP injury (TBI cluster)*

KCl-induced clusters of SD following LFP injury generated repeated episodes of hyperemia after each depolarization (Figure 4). The inter-SD level of rCBF gradually increased with recurrence of SDs ("*SD number*" effect in a repeated measures ANOVA, n = 12, $p < 0.001$, Figure 4). Meanwhile the intensity of the hyperemic response, measured by its AUC, decreased with recurrence of SDs ("*SD number*" effect in a repeated measures ANOVA, n = 12, p = 0.003, Figure 4).

$PbtO_2$ had repeated biphasic changes during each SD, similar to the pattern observed in the TBI-isolated group after spontaneous isolated SDs following LFP injury (Figure 4). The dip, peak, and inter-SD $PbtO_2$ levels did not differ from one SD to the next (no "*SD number*" effect in a repeated measures ANOVA, n = 6). $CMRO_2$ displayed constant transient increases during each SD (no "*SD number*" effect in a repeated measures ANOVA, n = 6). Inter-SD $CMRO_2$ gradually increased compared to baseline precluster levels ("*SD number*" effect in a repeated measures ANOVA, n = 6, $p < 0.001$, Figure 4).

[Glc]b decreased after each SD and was associated with biphasic [Lac]b changes (Figure 5). Neither inter-SD concentration nor [Glc]b dip, [Lac]b dip or increase were affected by the repetition (no "*SD number*" effect in a repeated measures ANOVA, n = 6 + 1 spontaneous cluster from group 2). The L/G displayed constant

transient increase during each depolarization (no "*SD number*" effect in a repeated measures ANOVA, n = 6 + 1 spontaneous cluster from group 2, Figure 5). We then compared the relationship between precluster L/G and L/G changes (ΔL/G = L/G after nine SDs—precluster L/G). Except for one animal with a high precluster L/G (9.3 due to a high [Lac]b = 1.9 mmol/l, purple outlier in Figure 5), ΔL/G was dependent on precluster L/G: the higher the precluster L/G, the greater the increase in L/G after the SD cluster ("*precluster L/G*" effect on log(ΔL/G) in a repeated measures ANOVA, n = 6, p = 0.018, Figure 5). ΔL/G was also closely related to [Glc]b values before the cluster: the lower the precluster

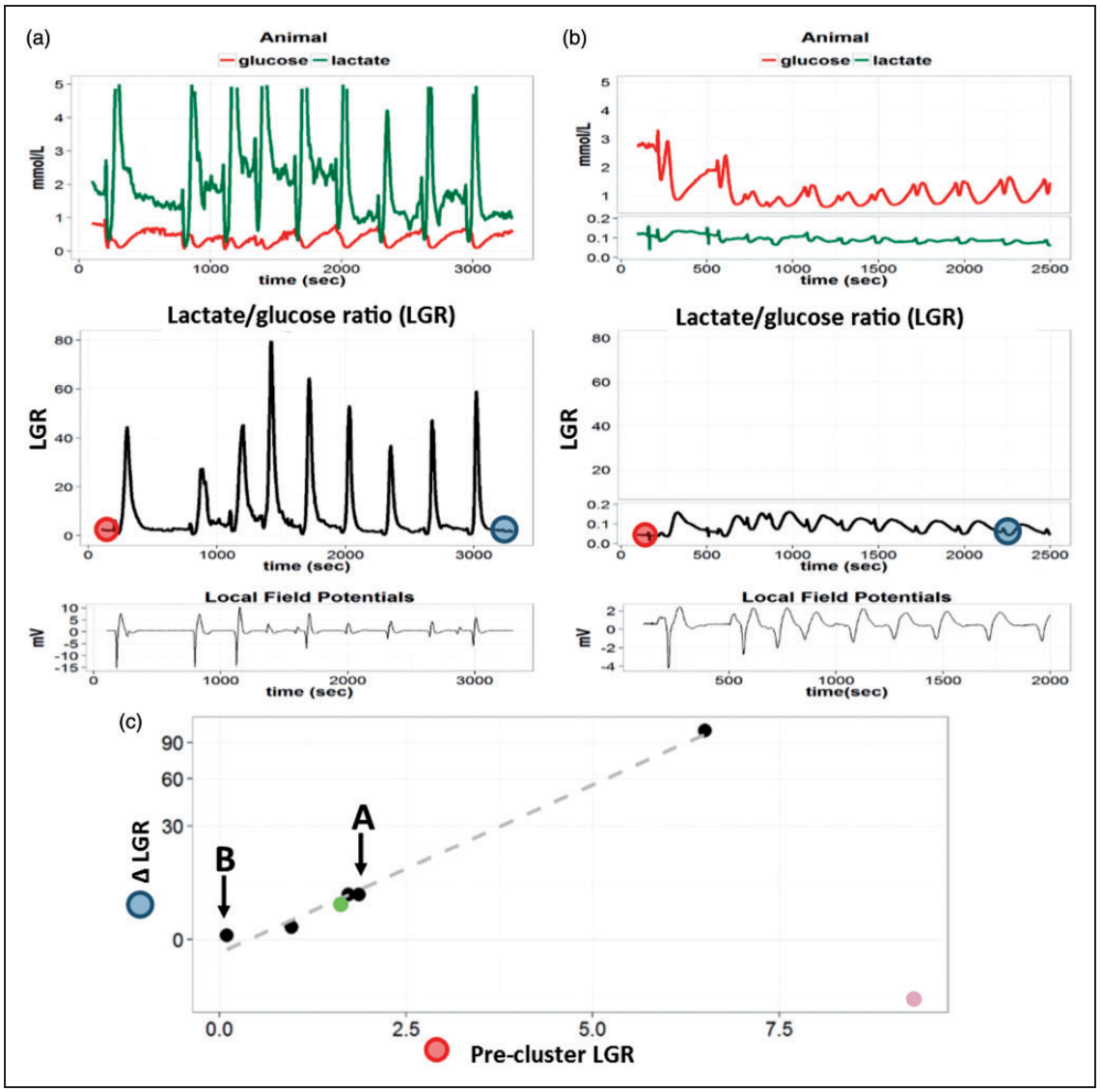


**Figure 5.** Changes in [Glc]b and [Lac]b during clusters of SDs in the injured brain. Animal A and B: Two examples of extracellular brain glucose ([Glc]b in mmol/L, red) and lactate ([Lac]b in mmol/L, green) concentration recordings. Below, the corresponding [Lac]b/[Glc]b ratio (LGR) is plotted in black. Repeated SDs in clusters can be visualized as slow DC shifts on the local field potential curve (near DC 0.02–0.5 Hz) in each animal. Panel C: ΔLGR = [LGR after the 9th SD (cf. dark blue circles in animal A and B)] − [precluster LGR (cf. red circles in animal A and B)]. The ΔLGR is plotted against precluster LGR (cf. red circles in animal A and B), with a logarithmic scale on the Y-axis. Each dot represents data from different animals (n = 6 + 1 spontaneous cluster of group 2, green dot). The dots corresponding to animals A and B are highlighted with black arrows. The gray dashed line represents the linear relation between log(ΔLGR) and precluster LGR, excluding an outlier (purple dot in the lower right corner with a high [Lac]b = 1.9 mmol/l and a high LGR). Note that the higher the precluster LGR, the greater the increase in LGR (ΔLGR) during the cluster (n = 6, p = 0.018, "*precluster LGR*" effect in a repeated measure ANOVA). A prolonged increase in LGR indicates failure in local oxidative energy metabolism.

[Glc]b, the higher the $\Delta L/G$ at the end of the cluster (''*precluster* [Glc]b'' effect on $\log(\Delta L/G)$ in a repeated measures ANOVA, $n = 6$, $p = 0.017$).

## Discussion

The present study described the metabolic and microvascular consequences of KCl-induced SDs in noninjured cortex, and of SDs occurring after severe LFP injury, either spontaneously or as a cluster evoked by KCl application following TBI.

We first identified SDs as a slow wave change in LFP.[8,38] SD was associated with a simultaneous transient hyperemic response characterized by an increase in LDF, as previously described. We then used minimally invasive techniques, including a 10 µm diameter oxygen sensor and 40 µm diameter biosensors, in order to monitor brain metabolism with minimal injury to the blood–brain barrier. The sensors provided a metabolic signature of SDs in noninjured brain that indicated an aerobic hyperglycolysis state (transient decrease in [Glc]b associated with transient increase in $PbtO_2$, rCBF and $CMRO_2$, and [Lac]b) recovering in 5–10 min. Severe LFP injury rapidly induced a consistent decrease in rCBF and [Glc]b in a cortical area known to degenerate seven days post-LFP injury, which we designated as a potential traumatic penumbra.[3] In this brain area at risk of neuronal injury, spontaneous SDs induced similar patterns of rCBF and [Glc]b changes to those observed in the control group, suggesting hypermetabolism. However, $PbtO_2$ and [Lac]b displayed an initial biphasic pattern followed by a prolonged decrease. Thus, 20 min after depolarization onset, [Lac]b and $PbtO_2$ remained lower than pre-SD levels in the traumatic penumbra, with a prolonged increase in $CMRO_2$. Thus, the traumatized brain parenchyma had not recovered its baseline metabolic values 20 min after SD onset. Finally, recurrent SDs in clusters were associated with a sustained increase in $CMRO_2$ and L/G. Taken together, these results indicate that SD triggered a hyperglycolysis state, in both noninjured and injured brain. However, the brain parenchyma exhibited altered responses to hyperglycolysis, with reduced hyperemia and no elevation in lactate concentration in TBI tissue as compared to noninjured cortex. These alterations could be at least partly responsible for the slower return to baseline metabolic values in traumatized brain challenged by SD.

### *TBI induces SDs in an early (5 h) posttraumatic time window*

TBI is a classic trigger of SD. Even minimal brain trauma using a pin with a diameter exceeding 50 µm is sufficient to induce SD.[39] Likewise, in animal models of TBI, the first impact triggers SD.[40–44] Further SDs may occur depending on TBI severity and metabolic imbalance.[42,45] However, their implication in secondary injury progression is controversial.[43,46] In the present study, severe LFP injury led to secondary spontaneous SDs in 80% of animals in the early time window between 30 min and 5 h postinjury. These findings are in line with clinical studies in which secondary SDs occurred in 50–60% of TBI patients.[10,22] Recordings in patients usually start later than the first 5 h postinjury (i.e. postsurgery). The time course of SD occurrence in rats is still unexplored, and it is difficult to extrapolate the number and incidence of SDs following TBI from animals to humans. Nonetheless, it is possible that the occurrence rate of SDs in patients could be higher than 50–60% if recordings started earlier.

Only one out of 12 animals showed a spontaneous cluster of recurrent SDs. However, it should be noted that SD occurrence was inhibited in our model, isoflurane being a well-established inhibitor of SD. For example, it was recently shown that isoflurane reduced the number of SDs in the early time window by 72% after middle cerebral artery occlusion.[47] Thus, more SD clusters might be observed in our LFP injury model under other types of anesthesia without inhibitory effect on SDs.

### *Hemodynamic responses to SD*

In rats and higher mammals including humans, spreading hyperemia is coupled to SD and is typically followed by oligemia under physiological conditions.[48,49] By contrast, an inverse neurovascular response is frequently observed in patients with TBI, aSAH, and MHS.[15,29,50] This inverse response is characterized by severe vasoconstriction and hypoperfusion up to ischemia instead of vasodilation and hyperemia.[8,21] The SD-triggered perfusion deficit spreads in the tissue together with the depolarization wave (=spreading ischemia), delaying the energy-dependent recovery from SD. If spreading ischemia is sufficiently prolonged, it leads to widespread cortical necrosis.[51] Spreading ischemia is an exceedingly complex phenomenon, involving dysregulation in all cell types of the neurovascular unit[8,49] and all segments of the vascular tree from large arteries[52] down to capillary level.[53] Spreading ischemia may start from a normal level of rCBF,[21] but a reduced level promotes it.[52,54] In animals, the phenomenon was observed in a model mimicking conditions present following aSAH[21] as well as models of global[55,56] and focal ischemia.[56–58]

Notably, the normal hyperemic and the inverse ischemic response to SD do not follow an ''all or

nothing'' principle: rather the hemodynamic response to SD changes along a continuum from hyperemic to terminal ischemic response with, intermediate biphasic patterns both in animals and patients.[52,56,59] It is noteworthy in this respect that a biphasic pattern of oxy- and deoxy-hemoglobin is already observed in models of focal ischemia when the rCBF response to SD shows a reduced but still monophasic increase.[56,60] This is probably due to the marked increase in $CMRO_2$ induced by SD, as previously reported[35] and confirmed in the present study. Such a biphasic pattern of oxy- and deoxyhemoglobin in the ischemic penumbra seems to correspond well to the biphasic $PbtO_2$ pattern, coupled to reduced monophasic increases in rCBF in the traumatic penumbra as observed here.

Interestingly, the normal monophasic $PbtO_2$ response to SD in naïve cortex in the present study differed markedly from the previously observed $PbtO_2$ response to SD in naïve cortex reported by Piilgaard and Lauritzen.[35] These authors described a very early peak of $PbtO_2$, which lasted for only 5–10 s. Notably, $PbtO_2$ then fell dramatically during physiological oligemia below the detection limit in some animals. It may be speculated that this discrepancy in results is related to a difference in anesthesia: isoflurane, as used in our study, markedly increases the rCBF level, to a range between 135 and 140 ml/100 g/min,[37,61] while anesthesia with α-chloralose, as used by Piilgaard and colleagues, markedly decreases the rCBF level to 53 ml/100 g/min.[62] A higher level of rCBF might allow more oxygen to be extracted. The same amount of extracted oxygen during SD could thus result in distinct $PbtO_2$ responses, depending on the baseline level of rCBF. Consistent with this hypothesis, the baseline level of $PbtO_2$ in the present experiments was 10 mmHg higher than the one in the experiments conducted by Piilgaard and Lauritzen.

Overall, it is possible that the reduced hyperemic response observed after TBI, compared to control animals, represents the initial part of a continuum from normal hyperemia to spreading ischemia.

### *Metabolic response to SD*

The normal metabolic response of a naïve brain to SD has already been extensively described using microdialysis, fluoro-deoxyglucose uptake, and autoradiography. SD evokes a transient decrease in [Glc]b coupled to an increase in [Lac]b and increased glucose consumption.[63–65] This response is typical of any metabolic challenge imposed on a normal brain and resembles that induced by electrical stimulation of neuronal activity.[66–69] Our biosensor's data are in good agreement with cMD in the normal or ischemic brain,[64,65] but the biosensors detected larger changes: [Glc]b decreased by ~63% and [Lac]b increased by 168%, compared with a 15–20% decrease and 60% increase, respectively, using cMD.[64,65] In addition, changes detected by microdialysis lasted longer than those detected by biosensors, especially in areas surrounding ischemic tissue.[70–72] We hypothesize that the small size of our microelectrode biosensors reduced the extent of brain injury caused by implantation compared to microdialysis probes and allowed more direct sampling of cerebral interstitial fluid. It is possible that a glial layer surrounding microdialysis probes added a diffusion barrier to the microdialysis membrane itself, resulting in low-pass filtering of fast neurochemical changes evoked by SDs. In addition, the biosensors allowed accurate estimation of [Glc]b and [Lac]b, which is difficult using microdialysis.

It is well established that normal metabolic response to SD involves glucose consumption and lactate release to sustain the energy requirements for neurons and glial cells to repolarize.[63,64,73] The increase in [Lac]b detected in the present study and by others is currently a matter of debate. It cannot be the result of increased diffusion from the bloodstream, because blood lactate concentration is below 1 mmol/l, which is less than [Lac]b.[74] Consequently, the concentration gradient rather indicates lactate diffusion out of the brain into the bloodstream. It has been suggested that lactate can be produced by glial cells and released into the extracellular fluid to serve as an alternative energy substrate for neurons.[69,75,76] However, other studies have estimated that this lactate release is only marginally consumed by brain cells, being mostly cleared out of the brain by the bloodstream.[64,77] Thus, elevated [Lac]b in response to SD is more likely the consequence of increased lactate production by the brain.

Our glucose and lactate monitoring experiments did not directly indicate the function of lactate release in response to SD. However, the absence of an increase in [Lac]b was one of the most striking differences between SDs evoked in control rats and those detected after TBI. Our results did not allow us to differentiate between impaired lactate production, increased lactate consumption, and accelerated clearance into the bloodstream. Since aerobic metabolism was preserved in the traumatic penumbra ($PtO_2$ and rCBF maintained, increase in $CMRO_2$), it is possible that the reduced numbers of glucose molecules involved in glycolysis entered the mitochondrial aerobic pathway, inducing reduced lactate production and release.[69,75,76] In addition, it can be speculated that, given the low [Glc]b level after TBI and the consequently limited energy supply, lactate released into the brain was utilized as an energy substrate to restore the ionic gradients disrupted by SD. Further studies are required to explore these hypotheses.

The biphasic $PbtO_2$ and [Lac]b changes that we observed are reminiscent of SD-induced biphasic Hb saturation changes that have been reported in the ischemic penumbra[56,78] and may correspond to a shift toward reduced nicotinamide adenine dinucleotide. Such SD-related redox changes have been reported during oxygen deficiency[79,80] or in patients with severe head injury.[81] Therefore, such a biphasic pattern might be a hallmark of metabolic imbalance. Overall, our experiments showed that the hypermetabolic response to SD seen in control rats was altered after TBI. In particular, the absence of [Lac]b elevation was associated with slower return to baseline $PbtO_2$ and $CMRO_2$ values, indicating that the metabolic challenge induced by SDs was more difficult to overcome after TBI.

### *Additional effects of clusters*

SD repetition within clusters has been recorded in patients and can last several hours.[6,12,13,22] Such clusters of SDs are associated with unfavorable outcome.[13,22] Here, clusters of SDs were evoked by continuous apposition of KCl at the cortical surface. Within these clusters, each SD induced metabolic changes similar to those induced by isolated SDs in the traumatic penumbra: transient repeated hyperemic events, increase in $CMRO_2$, and decrease in [Glc]b. However, with the repetition of 10 SDs within a cluster, a gradual increase in inter-SD rCBF was observed. Such prolonged [Glc]b and [Lac]b changes have also been reported during repeated SDs in aSAH or TBI patients.[71,82] Interestingly, there was a correlation between low precluster [Glc]b and increased L/G during the cluster. An increased L/G has often been associated with unfavorable outcome in clinical studies and is considered a marker of poor prognosis.[30,31] The present results suggest that SD clusters initiated in a traumatized cortical region already showing reduced [Glc]b may worsen the fate of the brain tissue, possibly by aggravating metabolic imbalance and neuronal loss.[6]

### *Limits*

Our experimental setup led to several limitations, due to respiratory assistance and anesthesia. Like all anesthetic compounds, isoflurane can affect basal brain metabolism and blood flow. For example, the low dose of isoflurane (0.8–1.5%) used as anesthetic agent is known to increase rCBF compared to $\alpha$-chloralose or ketamine.[36,37,62,83] Together with a slight increase in $PaCO_2$, our setup may have led to a ''luxury'' perfusion compared to experiments conducted under $\alpha$-chloralose anesthesia. Low dose isoflurane can also influence brain and systemic metabolism leading to an increase in blood and brain lactate concentrations.[84–86] These changes could be explained by the alteration of mitochondrial respiratory chain observed in neuronal cultured cells[87] and during heart preconditioning.[88] However, the pattern of brain glucose and lactate observed during SD in our study suggests a preserved mitochondrial function with an aerobic hyperglycolysis state. Clearly, ethical and technical issues limit the study of acute brain injury in awake animals. Such changes in brain metabolism induced by anesthesia should be taken into account when generalizing the findings obtained in animals.

In addition, more complete understanding of brain metabolism in control and traumatized animals should include pyruvate metabolism. For example, L/P is an important neurochemical index. In clinical studies, low L/P ($<40$) was associated with hyperglycolysis whereas $L/P > 40$ was indicative of metabolic crisis and poor patient outcome.[32,33] Including pyruvate biosensor monitoring is therefore an important challenge for future studies, to differentiate aerobic from anaerobic glycolytic patterns of metabolism.

### *A continuum from physiological hypermetabolic responses to metabolic crisis?*

The concept of a continuum, from normal hyperemic responses to SDs to pathological ischemic responses under conditions of brain injury, was recently proposed, including an array of intermediate biphasic patterns early in the course of neuronal degeneration.[52,56,59] In the present study, SDs that occurred spontaneously in the first 5 h following TBI displayed reduced hyperemia associated with altered hypermetabolic response, and slower return to baseline metabolic values. This vascular and metabolic signature may lie in the initial part of this continuum. The complete time course of SD occurrence in this model is currently unknown, but it is possible that, if SDs could be recorded later after TBI, as the traumatic penumbra evolves toward irreversible lesions, vascular and metabolic patterns could change along this continuum and display biphasic or ischemic profiles indicative of the evolution of neuronal injury. Further studies are required to explore this possibility.

## Funding

The author(s) disclosed receipt of the following financial support for the research, authorship, and/or publication of this article: Supported by the Hospices Civils de Lyon, Inserm and the Fondation Gueules cassées sourire quand même (FGC-11-2013 to SM), BB was supported by a PhD fellowship from Ecole de l'INSERM Bettencourt Schueller, Deutsche Forschungsgemeinschaft (DFG DR 323/6-1), the Bundesministerium für Bildung und Forschung (Center for

Stroke Research Berlin, 01 EO 0801) and Era-Net Neuron 01EW1212 to JPD.

## Acknowledgements

We are grateful to Lionel Bapteste for preliminary experiments and helpful discussions.

## Declaration of conflicting interests

The author(s) declared no potential conflicts of interest with respect to the research, authorship, and/or publication of this article.

## Authors' contribution

BB: designed and performed experiments, analyzed data, drafted and finalized the manuscript and approved the manuscript before submission.

AM: designed and performed experiments, contributed to and approved the manuscript before submission.

LB: contributed to and approved the manuscript before submission.

JPD: contributed to and approved the manuscript before submission.

SM: designed and performed experiments, contributed to and approved the manuscript before submission.

TL: designed and performed experiments, contributed to and approved the manuscript before submission.

## References

1. Cortez SC, McIntosh TK and Noble LJ. Experimental fluid percussion brain injury: vascular disruption and neuronal and glial alterations. *Brain Res* 1989; 482: 271–282.
2. McIntosh TK, Vink R, Noble L, et al. Traumatic brain injury in the rat: characterization of a lateral fluid-percussion model. *Neuroscience* 1989; 28: 233–244.
3. Balança B, Bapteste L, Lieutaud T, et al. Neuronal loss as evidenced by automated quantification of neuronal density following moderate and severe traumatic brain injury in rats. *J Neurosci Res* 2016; 94: 39–49.
4. von Oettingen G, Bergholt B, Gyldensted C, et al. Blood flow and ischemia within traumatic cerebral contusions. *Neurosurgery* 2002; 50: 781–788; discussion 788–790.
5. Somjen GG. Irreversible hypoxic (ischemic) neuron injury. In: Somjen GG (ed.) *Ions in the brain*. New York: Oxford University Press, 2004, pp.338–372.
6. Dreier JP and Reiffurth C. The stroke-migraine depolarization continuum. *Neuron* 2015; 86: 902–922.
7. Somjen GG. Mechanisms of spreading depression and hypoxic spreading depression-like depolarization. *Physiol Rev* 2001; 81: 1065–1096.
8. Dreier JP. The role of spreading depression, spreading depolarization and spreading ischemia in neurological disease. *Nat Med* 2011; 17: 439–447.
9. Lauritzen M, Dreier JP, Fabricius M, et al. Clinical relevance of cortical spreading depression in neurological disorders: migraine, malignant stroke, subarachnoid and intracranial hemorrhage, and traumatic brain injury. *J Cereb Blood Flow Metab* 2011; 31: 17–35.
10. Fabricius M, Fuhr S, Bhatia R, et al. Cortical spreading depression and peri-infarct depolarization in acutely injured human cerebral cortex. *Brain* 2006; 129: 778–790.
11. Hartings JA, Bullock MR, Okonkwo DO, et al. Spreading depolarisations and outcome after traumatic brain injury: a prospective observational study. *Lancet Neurol* 2011; 10: 1058–1064.
12. Dreier JP, Woitzik J, Fabricius M, et al. Delayed ischaemic neurological deficits after subarachnoid haemorrhage are associated with clusters of spreading depolarizations. *Brain* 2006; 129: 3224–3237.
13. Dreier JP, Major S, Pannek H-W, et al. Spreading convulsions, spreading depolarization and epileptogenesis in human cerebral cortex. *Brain* 2012; 135: 259–275.
14. Dohmen C, Sakowitz OW, Fabricius M, et al. Spreading depolarizations occur in human ischemic stroke with high incidence. *Ann Neurol* 2008; 63: 720–728.
15. Woitzik J, Hecht N, Pinczolits A, et al. Propagation of cortical spreading depolarization in the human cortex after malignant stroke. *Neurology* 2013; 80: 1095–1102.
16. Mody I, Lambert JD and Heinemann U. Low extracellular magnesium induces epileptiform activity and spreading depression in rat hippocampal slices. *J Neurophysiol* 1987; 57: 869–888.
17. Avoli M, Drapeau C, Louvel J, et al. Epileptiform activity induced by low extracellular magnesium in the human cortex maintained in vitro. *Ann Neurol* 1991; 30: 589–596.
18. Dreier JP, Kleeberg J, Petzold G, et al. Endothelin-1 potently induces Leão's cortical spreading depression in vivo in the rat: a model for an endothelial trigger of migrainous aura? *Brain* 2002; 125: 102–112.
19. Wei Y, Ullah G and Schiff SJ. Unification of neuronal spikes, seizures, and spreading depression. *J Neurosci* 2014; 34: 11733–11743.
20. von Bornstädt D, Houben T, Seidel JL, et al. Supply-demand mismatch transients in susceptible peri-infarct hot zones explain the origins of spreading injury depolarizations. *Neuron* 2015; 85: 1117–1131.
21. Dreier JP, Körner K, Ebert N, et al. Nitric oxide scavenging by hemoglobin or nitric oxide synthase inhibition by N-Nitro-L-arginine induces cortical spreading ischemia when K+ is increased in the subarachnoid space. *J Cereb Blood Flow Metab* 1998; 18: 978–990.
22. Hartings JA, Watanabe T, Bullock MR, et al. Spreading depolarizations have prolonged direct current shifts and are associated with poor outcome in brain trauma. *Brain* 2011; 134: 1529–1540.
23. Furlan M, Marchal G, Viader F, et al. Spontaneous neurological recovery after stroke and the fate of the ischemic penumbra. *Ann Neurol* 1996; 40: 216–226.
24. Baron JC. Perfusion thresholds in human cerebral ischemia: historical perspective and therapeutic implications. *Cerebrovasc Dis* 2001; 11: 2–8.
25. Cunningham AS, Salvador R, Coles JP, et al. Physiological thresholds for irreversible tissue damage in contusional regions following traumatic brain injury. *Brain* 2005; 128: 1931–1942.
26. Wu H-M, Huang S-C, Vespa P, et al. Redefining the pericontusional penumbra following traumatic brain injury: evidence of deteriorating metabolic derangements

based on positron emission tomography. *J Neurotrauma* 2013; 30: 352–360.
27. Zazulia AR, Diringer MN, Videen TO, et al. Hypoperfusion without ischemia surrounding acute intracerebral hemorrhage. *J Cereb Blood Flow Metab* 2001; 21: 804–810.
28. Claassen J, Perotte A, Albers D, et al. Nonconvulsive seizures after subarachnoid hemorrhage: multimodal detection and outcomes. *Ann Neurol* 2013; 74: 53–64.
29. Hinzman JM, Andaluz N, Shutter LA, et al. Inverse neurovascular coupling to cortical spreading depolarizations in severe brain trauma. *Brain* 2014; 137: 2960–2972.
30. Goodman J, Valadka A, Gopinath S, et al. Extracellular lactate and glucose alterations in the brain after head injury measured by microdialysis. *Crit Care Med* 1999; 27: 1965–1973.
31. Timofeev I, Carpenter KLH, Nortje J, et al. Cerebral extracellular chemistry and outcome following traumatic brain injury: a microdialysis study of 223 patients. *Brain* 2011; 134: 484–494.
32. Vespa P. Continuous EEG monitoring for the detection of seizures in traumatic brain injury, infarction, and intracerebral hemorrhage: 'to detect and protect'. *J Clin Neurophysiol* 2005; 22: 99.
33. Sahuquillo J, Merino M-A, Sánchez-Guerrero A, et al. Lactate and the lactate-to-pyruvate molar ratio cannot be used as independent biomarkers for monitoring brain energetic metabolism: a microdialysis study in patients with traumatic brain injuries. *PLoS One* 2014; 9: e102540.
34. Vasylieva N, Woeffler-Maucler C, Meiller A, et al. Immobilization method to preserve enzyme specificity in biosensors: consequences for brain glutamate detection. *Anal Chem* 2013; 85: 2507–2515.
35. Piilgaard H and Lauritzen M. Persistent increase in oxygen consumption and impaired neurovascular coupling after spreading depression in rat neocortex. *J Cereb Blood Flow Metab* 2009; 29: 1517–1527.
36. Poulsen P, Smith D, Østergaard L, et al. In vivo estimation of cerebral blood flow, oxygen consumption and glucose metabolism in the pig by [15O]water injection, [15O]oxygen inhalation and dual injections of [18F]fluorodeoxyglucose. *J Neurosci Methods* 1997; 77: 199–209.
37. Baughman V, Hoffman W, Thomas C, et al. Comparison of methohexital and isoflurane on neurologic outcome and histopathology following incomplete ischemia in rats. *Anesthesiology* 1990; 72: 85–94.
38. Fabricius M, Jensen L and Lauritzen M. Microdialysis of interstitial amino acids during spreading depression and anoxic depolarization in rat neocortex. *Brain Res* 1993; 612: 61–69.
39. Verhaegen MJ, Todd MM, Warner DS, et al. The role of electrode size on the incidence of spreading depression and on cortical cerebral blood flow as measured by $H_2$ clearance. *J Cereb Blood Flow Metab* 1992; 12: 230–237.
40. Nilsson P, Hillered L, Olsson Y, et al. Regional changes in interstitial K+ and Ca2+ levels following cortical compression contusion trauma in rats. *J Cereb Blood Flow Metab* 1993; 13: 183–192.
41. Zhang F, Sprague SM, Farrokhi F, et al. Reversal of attenuation of cerebrovascular reactivity to hypercapnia by a nitric oxide donor after controlled cortical impact in a rat model of traumatic brain injury. *J Neurosurg* 2002; 97: 963–969.
42. Rogatsky G, Sonn J and Kamenir Y. Relationship between intracranial pressure and cortical spreading depression following fluid percussion brain injury in rats. *J Neurotrauma* 2004; 20: 1315–1325.
43. Baumgarten L, Trabold R, Thal S, et al. Role of cortical spreading depressions for secondary brain damage after traumatic brain injury in mice. *J Cereb Blood Flow Metab* 2008; 28: 1353–1360.
44. Sato S, Kawauchi S, Okuda W, et al. Real-time optical diagnosis of the rat brain exposed to a laser-induced shock wave: observation of spreading depolarization, vasoconstriction and hypoxemia-oligemia. *PLoS One* 2014; 9: e82891.
45. Kubota M, Nakamura T, Sunami K, et al. Changes of local cerebral glucose utilization, DC potential and extracellular potassium concentration in experimental head injury of varying severity. *Neurosurg Rev* 1989; 12: 393–399.
46. Sword J, Masuda T, Croom D, et al. Evolution of neuronal and astroglial disruption in the peri-contusional cortex of mice revealed by in vivo two-photon imaging. *Brain J Neurol* 2013; 136: 1446–1461.
47. Takagaki M, Feuerstein D, Kumagai T, et al. Isoflurane suppresses cortical spreading depolarizations compared to propofol—implications for sedation of neurocritical care patients. *Exp Neurol* 2014; 252: 12–17.
48. Hadjikhani N, Sanchez Del Rio M, Wu O, et al. Mechanisms of migraine aura revealed by functional MRI in human visual cortex. *Proc Natl Acad Sci USA* 2001; 98: 4687–4692.
49. Ayata C and Lauritzen M. Spreading depression, spreading depolarizations, and the cerebral vasculature. *Physiol Rev* 2015; 95: 953–993.
50. Dreier JP, Major S, Manning A, et al. Cortical spreading ischaemia is a novel process involved in ischaemic damage in patients with aneurysmal subarachnoid haemorrhage. *Brain* 2009; 132: 1866–1881.
51. Dreier JP, Ebert N, Priller J, et al. Products of hemolysis in the subarachnoid space inducing spreading ischemia in the cortex and focal necrosis in rats: a model for delayed ischemic neurological deficits after subarachnoid hemorrhage? *J Neurosurg* 2000; 93: 658–666.
52. Feuerstein D, Takagaki M, Gramer M, et al. Detecting tissue deterioration after brain injury: regional blood flow level versus capacity to raise blood flow. *J Cereb Blood Flow Metab* 2014; 34: 1117–1127.
53. Østergaard L, Dreier JP, Hadjikhani N, et al. Neurovascular coupling during cortical spreading depolarization and depression. *Stroke* 2015; 46: 1392–1401.
54. Sukhotinsky I, Dilekoz E, Moskowitz MA, et al. Hypoxia and hypotension transform the blood flow response to cortical spreading depression from hyperemia into hypoperfusion in the rat. *J Cereb Blood Flow Metab* 2008; 28: 1369–1376.

55. Farkas E, Pratt R, Sengpiel F, et al. Direct, live imaging of cortical spreading depression and anoxic depolarisation using a fluorescent, voltage-sensitive dye. *J Cereb Blood Flow Metab* 2008; 28: 251–262.
56. Bere Z, Obrenovitch TP, Kozák G, et al. Imaging reveals the focal area of spreading depolarizations and a variety of hemodynamic responses in a rat microembolic stroke model. *J Cereb Blood Flow Metab* 2014; 34: 1695–1705.
57. Shin HK, Dunn AK, Jones PB, et al. Vasoconstrictive neurovascular coupling during focal ischemic depolarizations. *J Cereb Blood Flow Metab* 2006; 26: 1018–1030.
58. Strong AJ, Anderson PJ, Watts HR, et al. Peri-infarct depolarizations lead to loss of perfusion in ischaemic gyrencephalic cerebral cortex. *Brain* 2007; 130: 995–1008.
59. Offenhauser N, Windmüller O, Strong AJ, et al. The gamut of blood flow responses coupled to spreading depolarization in rat and human brain: from hyperemia to prolonged ischemia. *Acta Neurochir Suppl* 2011; 110: 119–124.
60. Dreier JP, Kleeberg J, Alam M, et al. Endothelin-1-induced spreading depression in rats is associated with a microarea of selective neuronal necrosis. *Exp Biol Med* 2007; 232: 204–213.
61. Linde R, Schmalbruch IK, Paulson OB, et al. The Kety-Schmidt technique for repeated measurements of global cerebral blood flow and metabolism in the conscious rat. *Acta Physiol Scand* 1999; 165: 395–401.
62. Zhu X-H, Zhang Y, Tian R-X, et al. Development of 17O NMR approach for fast imaging of cerebral metabolic rate of oxygen in rat brain at high field. *Proc Natl Acad Sci USA* 2002; 99: 13194–13199.
63. Adachi K, Cruz NF, Sokoloff L, et al. Labeling of metabolic pools by [6-14C]glucose during K(+)-induced stimulation of glucose utilization in rat brain. *J Cereb Blood Flow Metab* 1995; 15: 97–110.
64. Feuerstein D, Backes H, Gramer M, et al. Regulation of cerebral metabolism during cortical spreading depression. *J Cereb Blood Flow Metab*. Epub ahead of print 28 October 2015. DOI: 10.1177/0271678X15612779.
65. Hashemi P, Bhatia R, Nakamura H, et al. Persisting depletion of brain glucose following cortical spreading depression, despite apparent hyperaemia: evidence for risk of an adverse effect of Leão's spreading depression. *J Cereb Blood Flow Metab* 2009; 29: 166–175.
66. Kuhr W, van den Berg C and Korf J. In vivo identification and quantitative evaluation of carrier-mediated transport of lactate at the cellular level in the striatum of conscious, freely moving rats. *J Cereb Blood Flow Metab* 1988; 8: 848–856.
67. Krugers H, Jaarsma D and Korf J. Rat hippocampal lactate efflux during electroconvulsive shock or stress is differently dependent on entorhinal cortex and adrenal integrity. *J Neurochem* 1992; 58: 826–830.
68. Hu Y and Wilson G. A temporary local energy pool coupled to neuronal activity: fluctuations of extracellular lactate levels in rat brain monitored with rapid-response enzyme-based sensor. *J Neurochem* 1997; 69: 1484–1490.
69. Simpson IA, Carruthers A and Vannucci SJ. Supply and demand in cerebral energy metabolism: the role of nutrient transporters. *J Cereb Blood Flow Metab* 2007; 27: 1766–1791.
70. Hopwood SE, Parkin MC, Bezzina EL, et al. Transient changes in cortical glucose and lactate levels associated with peri-infarct depolarisations, studied with rapid-sampling microdialysis. *J Cereb Blood Flow Metab* 2005; 25: 391–401.
71. Feuerstein D, Manning A, Hashemi P, et al. Dynamic metabolic response to multiple spreading depolarizations in patients with acute brain injury: an online microdialysis study. *J Cereb Blood Flow Metab* 2010; 30: 1343–1355.
72. Gramsbergen JB, Skjøth-Rasmussen J, Rasmussen C, et al. On-line monitoring of striatum glucose and lactate in the endothelin-1 rat model of transient focal cerebral ischemia using microdialysis and flow-injection analysis with biosensors. *J Neurosci Methods* 2004; 140: 93–101.
73. Rogers ML, Feuerstein D, Leong CL, et al. Continuous online microdialysis using microfluidic sensors: dynamic neurometabolic changes during spreading depolarization. *ACS Chem Neurosci* 2013; 4(5): 799–807.
74. Gobatto CA, de Mello MA, Sibuya CY, et al. Maximal lactate steady state in rats submitted to swimming exercise. *Comp Biochem Physiol A Mol Integr Physiol* 2001; 130: 21–27.
75. Magistretti P and Pellerin L. Cellular bases of brain energy metabolism and their relevance to functional brain imaging: evidence for a prominent role of astrocytes. *Cereb Cortex* 1996; 6: 50–61.
76. Bélanger M, Allaman I and Magistretti PJ. Brain energy metabolism: focus on astrocyte-neuron metabolic cooperation. *Cell Metab* 2011; 14: 724–738.
77. Cruz NF, Adachi K and Dienel GA. Rapid efflux of lactate from cerebral cortex during K+-induced spreading cortical depression. *J Cereb Blood Flow Metab* 1999; 19: 380–392.
78. Wolf T, Lindauer U, Reuter U, et al. Noninvasive near infrared spectroscopy monitoring of regional cerebral blood oxygenation changes during peri-infarct depolarizations in focal cerebral ischemia in the rat. *J Cereb Blood Flow Metab* 1997; 17: 950–954.
79. Takano T, Tian G-FF, Peng W, et al. Cortical spreading depression causes and coincides with tissue hypoxia. *Nat Neurosci* 2007; 10: 754–762.
80. Sonn J and Mayevsky A. Responses to cortical spreading depression under oxygen deficiency. *Open Neurol J* 2012; 6: 6–17.
81. Mayevsky A, Doron A, Manor T, et al. Cortical spreading depression recorded from the human brain using a multiparametric monitoring system. *Brain Res* 1996; 740: 268–274.
82. Sakowitz OW, Santos E, Nagel A, et al. Clusters of spreading depolarizations are associated with disturbed cerebral metabolism in patients with aneurysmal subarachnoid hemorrhage. *Stroke J Cereb Circ* 2013; 44: 220–223.
83. Hyder F, Kennan R, Kida I, et al. Dependence of oxygen delivery on blood flow in rat brain: a 7 tesla nuclear magnetic resonance study. *J Cereb Blood Flow Metab* 2000; 20: 485–498.

84. Makaryus R, Lee H, Yu M, et al. The metabolomic profile during isoflurane anesthesia differs from propofol anesthesia in the live rodent brain. *J Cereb Blood Flow Metab* 2011; 31: 1432–1442.
85. Boretius S, Tammer R, Michaelis T, et al. Halogenated volatile anesthetics alter brain metabolism as revealed by proton magnetic resonance spectroscopy of mice in vivo. *NeuroImage* 2013; 69: 244–255.
86. Horn T and Klein J. Lactate levels in the brain are elevated upon exposure to volatile anesthetics: a microdialysis study. *Neurochem Int* 2010; 57: 940–947.
87. Yang Y, Chen X, Min H, et al. Persistent mitoKATP activation is involved in the isoflurane-induced cytotoxicity. *Mol Neurobiol*. Epub ahead of print 23 January 2016. DOI: 10.1007/s12035-016-9710-z.
88. Agarwal B, Dash RK, Stowe DF, et al. Isoflurane modulates cardiac mitochondrial bioenergetics by selectively attenuating respiratory complexes. *Biochim Biophys Acta* 2014; 1837: 354–365.